

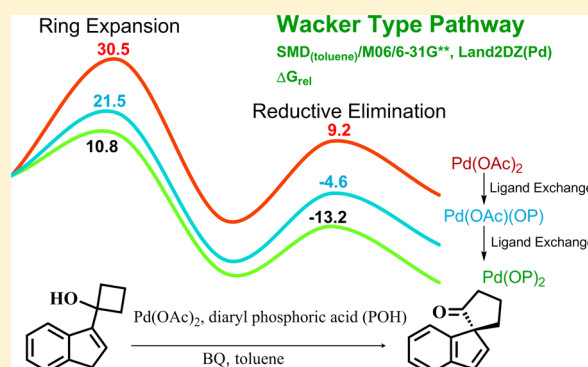
Importance of Ligand Exchanges in Pd(II)-Brønsted Acid Cooperative Catalytic Approach to Spirocyclic Rings

Garima Jindal and Raghavan B. Sunoj*

Indian Institute of Technology Bombay, Powai, Mumbai, Maharashtra 400076, India

S Supporting Information

ABSTRACT: Increasing number of reports in the most recent literature convey the use of palladium and Brønsted acids as cooperative catalytic partners. However, the mechanistic understanding of several such cooperative catalytic reactions and the origin of cooperativity continue to remain limited. In transition metal catalysis, it is typically assumed that the native ligands, such as the acetates in palladium acetate, are retained throughout the catalytic cycle. Herein, we convey the significance of invoking ligand exchanges in transition metal catalysis by using the mechanism of a representative cooperative dual-catalytic reaction. Density functional theory (M06 and B3LYP) computations have been employed to decipher the mechanism of Pd(II)-Brønsted acid catalyzed migratory ring expansion reaction of an indenyl cyclobutanol to a spirocyclic indene bearing a quaternary carbon. The molecular role of water, benzoquinone and phosphoric acid has been probed by computing the energetics using several combinations of all these as ligands on palladium. Of the two key mechanistic possibilities examined, a Wacker-type pathway (involving a semipinacol ring expansion of cyclobutanol followed by a reductive elimination) is found to be energetically more preferred over an allylic pathway wherein the ring expansion in a Pd- π -allyl intermediate occurs subsequent to the initial allylic C–H activation. The Gibbs free energies of the transition states with the native palladium acetate are much higher than a Pd-*bis*-phosphate species generated through ligand exchanges.



INTRODUCTION

The activation of inert and ubiquitous C–H bonds by using transition metal catalysts has gained widespread acceptance both in industry and academia.¹ The contemporary developments in C–H activation reactions reveal an overwhelming trend toward the use of multiple catalysts under one-pot reaction conditions.² Incredibly interesting demonstrations on cooperative catalysis, harnessing the potential of two or more catalysts, have become conspicuously more prominent in the most recent times.³ Quite naturally, the mechanistic picture gets increasingly more complex with the increase in the number of catalysts, additives, and reactants. Hence, the mechanistic underpinnings of cooperative multicatalytic reactions deserve diligent and urgent attention in view of its rapid progress.

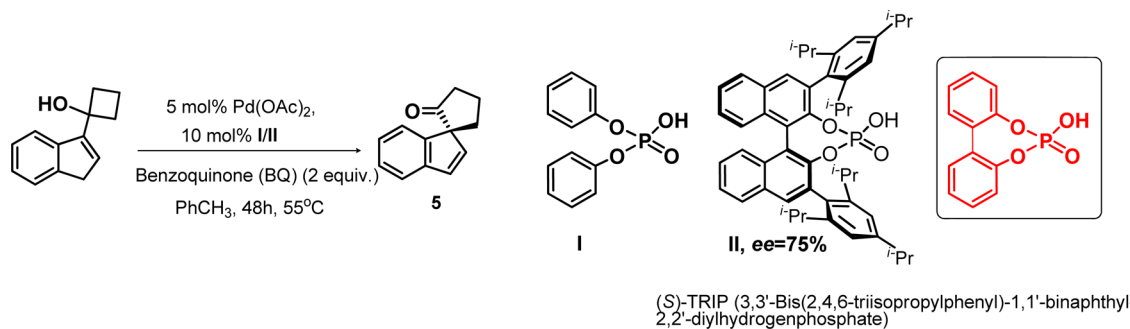
The key challenges toward developing improved mechanistic clarity relates to the lack of knowledge on the sheer number of possibilities for the catalytically active species, the sequence of action of each catalyst on the substrate, and energetic details of various steps in the catalytic cycle and so on. In particular, exchange of the native ligands on the transition metal by other ligands or additives, commonly considered as spectator/innocent ligands, opens up a myriad of possibilities. Although to a limited extent, ligand exchange has indeed been invoked in some transition metal catalyzed reactions.⁴ For instance, in a recent study by Houk and co-workers, the role of amino acid

ligands in a palladium acetate catalyzed remote C–H activation was investigated.^{4c} Deprotonation of the amino acid ligand by the palladium-bound acetate was suggested to lead to the formation of a neutral acetic acid molecule. The labile acetic acid thus makes way to the incoming substrate while the amino acid carboxylate binds to palladium. In another example by the Sanford group, a chloride is considered as exchanged with an acetate or an azide ligand. The resulting complexes were characterized using NMR and X-ray crystallography.^{4d} Herein, we intend to disclose how important it is to consider the exchange of labile ligands through the catalytic cycle in a cooperative multicatalytic situation. Whereas the chosen example in this study is expected to contribute to an improved view in the way such mechanistic scenarios are perceived at the molecular level, the results could have much wider implications in the burgeoning area of cooperative catalysis.⁵

Recently, Rainey and co-workers reported the first asymmetric C–C bond formation reaction employing an allylic C–H activation reaction (Scheme 1).⁶ While the examples on allylic C–H activation have been rich and abundant,⁷ the corresponding asymmetric versions remained generally scarce.⁸ The chiral induction is achieved by using a chiral Brønsted acid

Received: July 28, 2014

Published: October 27, 2014

Scheme 1. Palladium and Brønsted Acid Cooperative Catalytic Method for the Formation of Spirocyclic Indenes^{6,a}

^aA model phosphoric acid, shown in the inset, is used in our mechanistic investigation.

(S)-TRIP (**II**) in place of an achiral diphenyl phosphate (**I**). This reaction not only offers access to an interesting class of spirocyclic compound bearing a quaternary chiral carbon, it also constitutes an exquisite example of cooperative catalysis.³ Synthesis of spirocyclic frameworks consisting of quaternary carbons is generally a difficult task.⁹ It is worth reckoning that spirocyclic indenenes, such as that in antitumor drug fredericamycin A and anti-amnesic drug acutumine are valuable structural motifs owing to their biological activity.¹⁰

Phosphoric acid and Pd(II) catalysts have been used together in a few interesting reactions.¹¹ An oxo-Diels–Alder reaction employing a Pd(II)-Brønsted acid dual cooperative catalysis approach yielded products only when both catalysts were present.¹² A very recent allylic C–H activation employed a Pd(II)-phosphoric acid combination toward realizing a series of oxazolidinones.¹³ In another report, an allylic C–H amination has been demonstrated to exhibit significant dependence on the presence of water.¹⁴ Similarly, one of the ubiquitous oxidants in transition metal catalysis, namely benzoquinone (BQ), is also proposed to function as a ligand under certain reaction conditions.¹⁵ In an one-pot reaction as in the present example, the catalyst, cocatalyst Brønsted acid (abbreviated as POH hereafter), oxidant BQ, and water are all present in the reaction mixture. More importantly, the reaction was sluggish in the absence of any one of the above species in addition to the catalysts. In view of these important observations, it appears evident that deriving meaningful mechanistic insights would demand explicit consideration of the role of each species in the reaction.

Besides these general mechanistic details, a few pertinent questions are of high timely relevance to the rapidly emerging domain of cooperative catalysis. These include (a) whether or not the transition metal catalyst and Brønsted acid catalyst operate in a cooperative fashion? (b) What are the molecular role of phosphoric acid (POH), the cocatalyst/oxidant (BQ), and water? (c) whether the mechanism follows a Wacker type pathway or an allylic C–H activation? Whereas both mechanisms can be regarded as quite likely, there are only very few examples in literature where there is a consensus on the actual pathway followed under similar situations.¹⁶ Improved insights on the mechanism would help exploit the scope of asymmetric variants of such reactions. In view of these intriguing questions as well as in keeping with our continued interest toward understanding the mechanism of transition metal and Brønsted acid catalyzed reactions,¹⁷ we became interested in examining the mechanism of the title reaction. Herein, we employ density functional theory tools (M06 and B3LYP) to shed light on the nature of the potential active

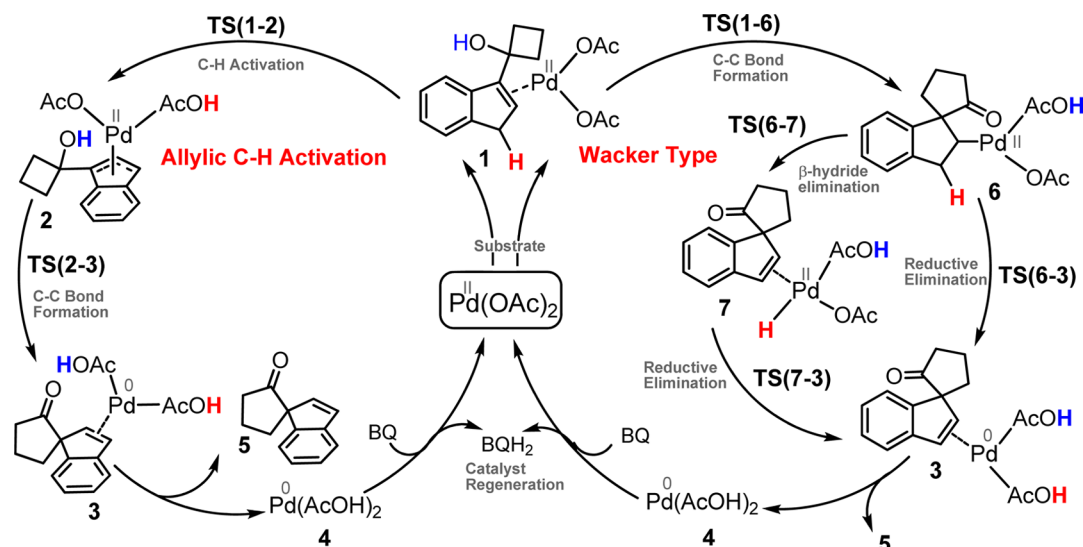
species, key intermediates and transition states involved in the reaction. In line with the literature precedence, a model catalyst as shown in the inset of Scheme 1 has been chosen for our mechanistic investigation.

■ COMPUTATIONAL METHODS

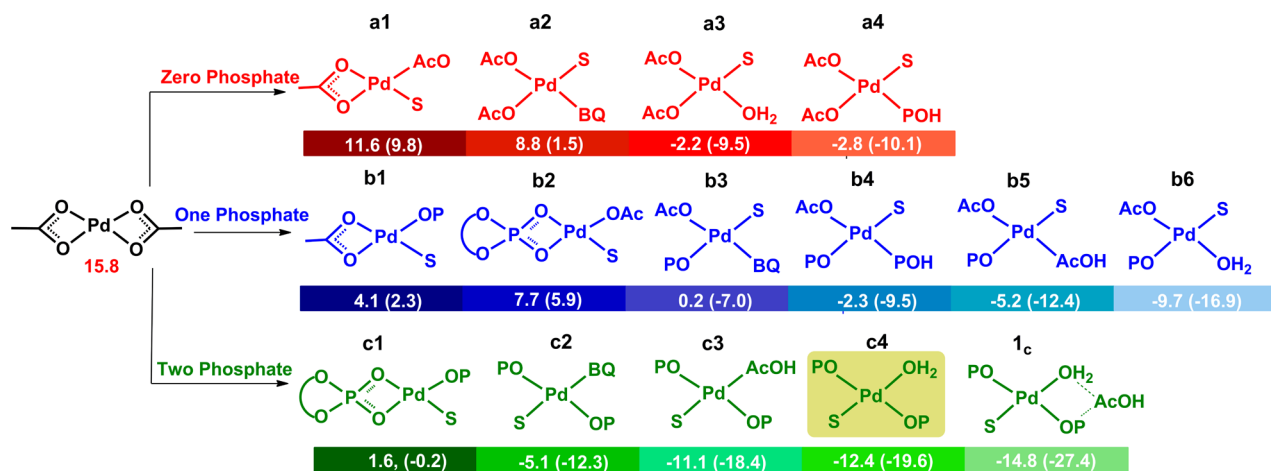
Computations were performed using Gaussian09 suite of quantum chemical program.¹⁸ The geometries were first optimized using the B3LYP hybrid density functional theory using Pople's 6-31G** basis set for all atoms except Pd.¹⁹ The LANL2DZ basis set consisting of an effective core potential (ECP) for 28 core electrons and a double- ζ quality valence basis set for 18 valence electrons was used for palladium.²⁰ All the stationary points were characterized, as minima or a first-order saddle point (transition states) by evaluating the corresponding Hessian indices. The transition states were verified as possessing a unique imaginary frequency in accordance with the anticipated reaction coordinate. Intrinsic reaction coordinate (IRC) calculations were additionally carried out to ascertain the true nature the transition states.²¹ The geometries obtained as the end-points on either side of the IRC trajectories were subjected to further optimization using a more stringent criteria by using "opt = calcfc" (as implemented in Gaussian09 program). This exercise enabled us to obtain the reactant and product such that their connection to the transition state could be established.

Single-point energies were calculated at the SMD_(Toluene)/M06/6-31G**, LANL2DZ(Pd) and the SMD_(Toluene)/M06/6-311G**, LANL2DZ(Pd) levels of theory using the B3LYP/6-31G**, LANL2DZ(Pd) geometries.²² The M06 functional has been widely used in recent literature to account for noncovalent interactions in transition metal systems.²³ The effect of a solvent continuum, in toluene, was evaluated using the Cramer–Truhlar continuum solvation model that employs quantum mechanical charge density of solutes, designated as SMD.²⁴ The zero-point vibrational energy (ZPVE), thermal, and entropic corrections obtained at 298.15 K and 1 atm pressure derived from the gas phase computations at the B3LYP/6-31G**, LANL2DZ(Pd) level of theory have been applied to the "bottom-of-the-well" energies obtained from the single-point energy evaluations in the solvent phase at the M06 functional to estimate the Gibbs free energies of solutes in the condensed phase.

Although the above-mentioned estimates of Gibbs free energies that are generally employed should be regarded as effective for comparison of relative free energies, it is known that entropy in the solution phase is inadequately described due to the suppression of translational entropy upon moving from the gas phase to a solvent. Thus, the Sackur–Tetrode equation, which is otherwise used to calculate the translational entropy cannot directly be applied in the solution phase. However, there are no accurate methods available to account for this deficiency. Hence, different methods have been recommended to correct the entropic contributions arising out of translational motion. In some studies the translational contribution to entropy is completely neglected,²⁵ whereas corrections were added to the free energies using the free volume theory in a few other reports.²⁶ As an extension of the

Scheme 2. Two Different Mechanistic Possibilities for the Formation of Spirocyclic Indene (5)^a

^aThis is only a representative scheme with the native Pd(OAc)₂ as the catalyst. For sake of simplicity, the notations are retained in various other possibilities arising due to ligand exchanges as described in the text.



S=Substrate, AcO=Acetate, PO=Phosphate, AcOH=Acetic acid, POH=Phosphoric acid, BQ=Benzoquinone

Figure 1. Gibbs free energies (kcal/mol) of formation of different likely active species computed with respect to the separated reactants (substrate, Pd₃(OAc)₆, BQ, POH, AcOH and H₂O).³³ The values in parentheses correspond to relative free energies (kcal/mol) inclusive of translational entropy corrections obtained using the Whitesides method.²⁷

free volume theory of solutions, Whitesides and co-workers have developed an interesting formulation, wherein corrections are made to the Sackur–Tetrode equation on the basis of the molecular volume.²⁷ We have calculated the corrected free energies by including entropic contributions by using the Whitesides method in view of different number of species are involved in the present work.²⁸ Furthermore, the lowest energy stationary points in the catalytic cycles were subjected to full geometry optimization at the SMD_(Toluene)/M06/6-31G**/LANL2DZ(Pd) level of theory. The energetic trends are found to be similar to that obtained using single point energy calculations.²⁹ The discussions in the text are presented using the SMD_(Toluene)/M06/6-31G**/LANL2DZ(Pd)//B3LYP/6-31G**/LANL2DZ(Pd) level of theory.

RESULTS AND DISCUSSION

Two most likely mechanistic possibilities are shown in Scheme 2, which proceed either through (a) an allylic C–H activation or (b) a Wacker type process. In the former case, an allylic C–

H bond in the initial catalyst-substrate complex (1) is activated first, via TS(1–2), to give a Pd- π -allyl intermediate 2. This is followed by a semipinacol type rearrangement involving the ring expansion of the cyclobutanol to a spirocyclic intermediate 3. The corresponding transition state for the C–C bond formation TS(2–3) revealed a concomitant reductive elimination facilitated by the transfer for a proton from the cyclobutanol OH group to the Pd-bound acetate. In the Wacker type pathway, a semipinacol ring expansion in 1 occurs first via TS(1–6). The resulting intermediate (6) can undergo either an acetate-assisted deprotonation (via TS(6–3)) to directly yield the product complex (3) in a single step or a β -hydride elimination first to give a Pd-hydride intermediate (7) followed by a reductive elimination to furnish 3. In both these pathways, the release of the final product (5) and the accompanying oxidation of Pd(0) to Pd(II) by benzoquinone (BQ) can sustain the catalytic cycle.³⁰

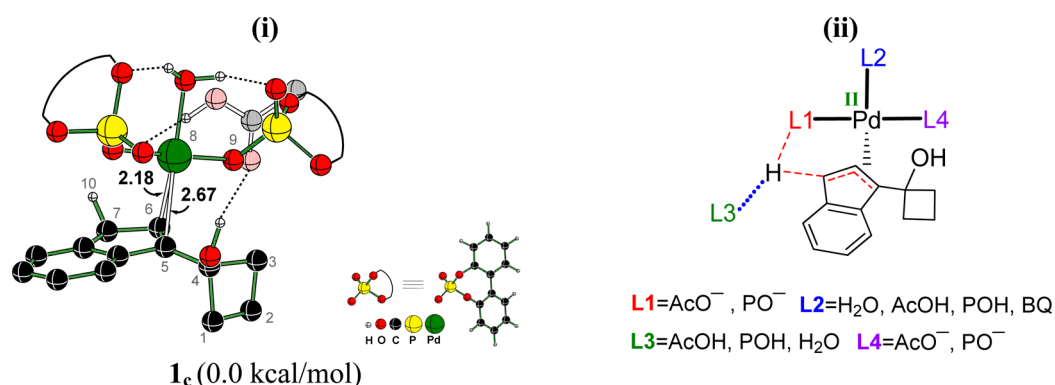


Figure 2. (i) Optimized geometry of complex $[\text{Pd}(\text{OP})_2(\text{S})(\text{H}_2\text{O})]$ with one AcOH (1_c). Distances are given in Å. Only select hydrogens are shown for improved clarity. The explicit AcOH is shown in a lighter shade. (ii) Different ligand combinations considered for the allylic C–H activation transition state $\text{TS}(1-2)$.

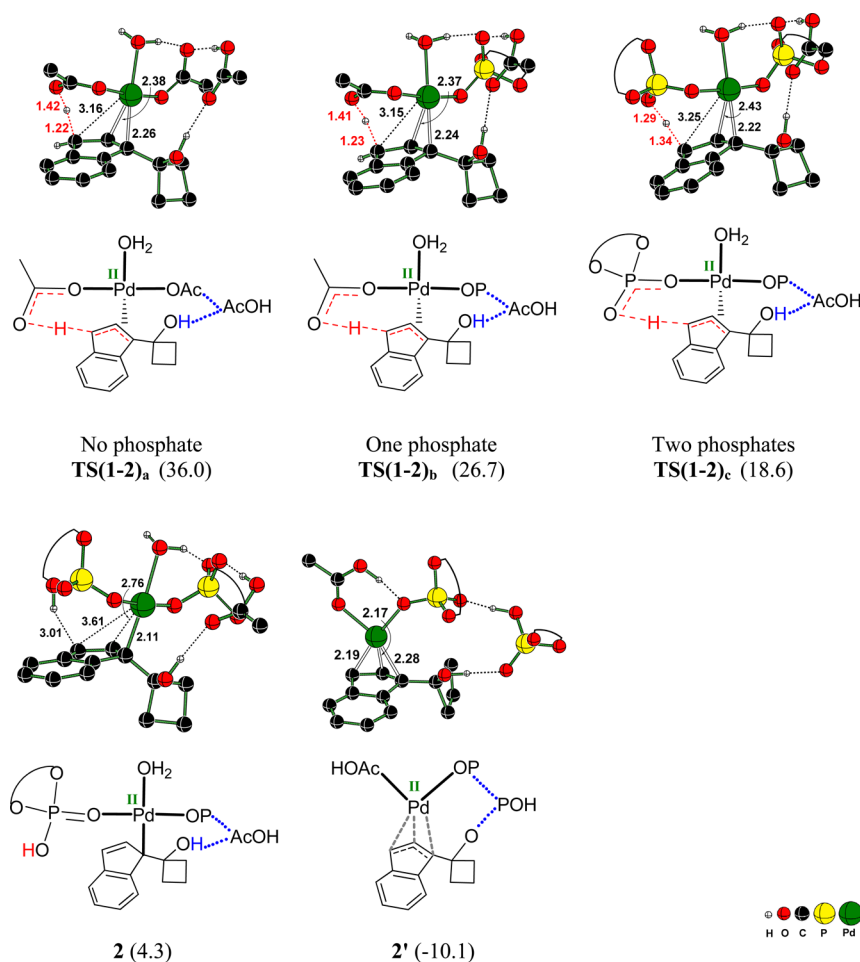


Figure 3. Optimized geometries of the lower energy transition states for the ligand-assisted C–H activation with zero, one and two phosphate ligands and the intermediates 2 and $2'$. Relative free energies (kcal/mol) are given in parentheses. All distances are in Å. The reaction coordinate and H-bonding are shown, respectively, in red and blue colors.

Ligand Exchange. We envisaged an active role of Brønsted acid (POH), benzoquinone (BQ), and H_2O in the individual catalytic steps. The conventional pathway promoted by $\text{Pd}(\text{OAc})_2$ is shown in Scheme 2. The substrate (S), POH , BQ and H_2O can as well bind to Pd via ligand exchanges. The acetate ligand on palladium can be protonated by the phosphoric acid, resulting in the formation of an acetic acid and a phosphate anion. While phosphate ion can coordinate to palladium, the neutral and labile acetic acid on palladium can

open up a cascade of ligand exchange possibilities with other neutral ligands. In fact, a similar protonation of acetate ligands by a phosphoryl directing group and subsequent removal of an acetic acid has been recently shown in a Pd and Rh catalyzed C–H activation reaction.³¹ The thermodynamic feasibility of such ligand exchanges leading to the formation of several other potential catalytic species is summarized in Figure 1.³² Interestingly, the conversion of the native $\text{Pd}(\text{OAc})_2$ to a number of other species is found to be exergonic wherein Pd is

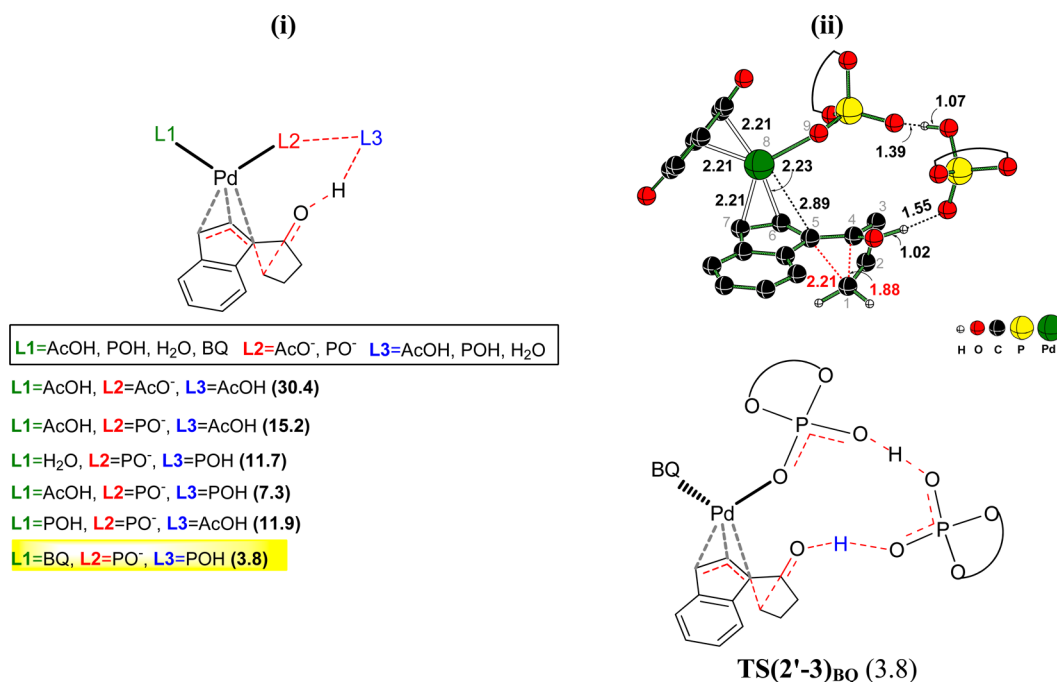


Figure 4. (i) Different likely ligand combinations in the C–C bond formation transition state TS(2'-3). All ligand combinations considered are provided in the inset, while the relative Gibbs free energies (kcal/mol) of the important TSs are given in parentheses. (ii) The lowest energy TS TS(2'-3)_{BQ} involving BQ as a ligand. All distances are in Å, and the relative free energy (kcal/mol) is provided in parentheses. The reaction coordinate is shown in red color dashed lines.

bound to the substrate as well as to other ligands. The lower energy possibilities are identified as the ones with two phosphates as shown using green highlighting in Figure 1.

The energetically most favorable *bis*-phosphate complex ([Pd(OP)₂(OH₂)S], as shown in the inset) is further optimized by explicitly including an acetic acid molecule which is expected to be generated by the protonation of the native Pd-bound acetate by POH in the ligand exchange process. In the formation of Pd complex involving two phosphate molecules, two molecules of AcOH will be generated. The second AcOH molecule only plays a passive role.³⁴ The resulting lowest energy complex, designated as 1_c (Figure 2(i)), is henceforth taken as the reference point for comparison of energies in this study. A similar kind of ligand exchange can as well occur during the individual steps, such as the C–H activation, reductive elimination and so on. Therefore, we have investigated the complete catalytic cycle (as shown in Scheme 2) with all likely ligand combinations so as to identify the lowest energy TSs in each of the elementary step. In addition to the inner-sphere ligands directly bound to the metal (denoted as L1, L2, and L4), an auxiliary outer-sphere ligand (L3) held by hydrogen bonding interaction is also taken into consideration (Figure 2(ii)). This approach would help identify the best ligand combination for the different steps involved in the catalytic cycle.

Allylic C–H Activation Pathway. (i). *C–H Activation.* The TS for the allylic C–H bond activation is located, first with the native Pd(OAc)₂ catalyst (TS(1–2)_a). Consideration of various ligands as in Figure 2(ii), conveys that water is relatively more preferred inner-sphere ligand when the other two ligands on Pd are κ¹ acetates.³⁵ Subsequent replacement of the acetates with phosphate ligands (TS(1–2)_b and TS(1–2)_c) resulted in further lowering of energy of the C–H bond activation TS. The geometries of these TSs (Figure 3) indicate that the substrate

maintains an η² coordination with Pd, while AcO⁻ and PO⁻ are bound in a κ¹ coordination mode. Transition states with η³ coordination are found to be of higher energy.³⁶ Certain interesting features arising due to the ligand exchange are evident at this juncture. For instance, the Gibbs free energy of the TS for the acetate-assisted C–H activation (TS(1–2)_a) is about 17 kcal/mol higher as compared to the corresponding phosphate-assisted analogue (TS(1–2)_c). In TS(1–2)_a an additional molecule of AcOH is included to enable a balanced comparison between different TSs (namely, TS(1–2)_a, TS(1–2)_b and TS(1–2)_c). Equally important is to note that AcOH has also been used as an additive together with phosphoric acid in the experimental study.⁶ While there have been numerous reports on acetate-assisted C–H activation,^{17a,c,d,37} an equivalent role of Pd-bound phosphates have not been reported yet. This is an interesting prediction which could have wider implications in transition metal catalysis in the presence of phosphate ligands.^{11–13} Equally significant is to note that Pd-phosphates have even been suggested as active catalytic species under certain reactions.^{13,38}

(ii). *Ring Expansion.* Intermediate 2 formed as a result of the C–H activation exhibits an η¹ coordination of the substrate with palladium (Figure 3). It is identified that the dissociation of one of the neutral labile ligands (H₂O) leads to the formation of a Pd η³ complex (2'). More importantly, intermediate 2' is found to be of lower energy than 2.³⁹ The next step in the allylic pathway is the C–C bond formation resulting in ring expansion via TS(2'-3) to the spirocyclic product (5). Since this is the stereodetermining step that controls the sense of the developing chirality at the quaternary carbon, the knowledge of the actual catalytic species can greatly benefit in the development of asymmetric reactions. Akin to the steps described previously, TS(2'-3) with varying inner-sphere and outer-sphere ligands are considered. It can be noted from

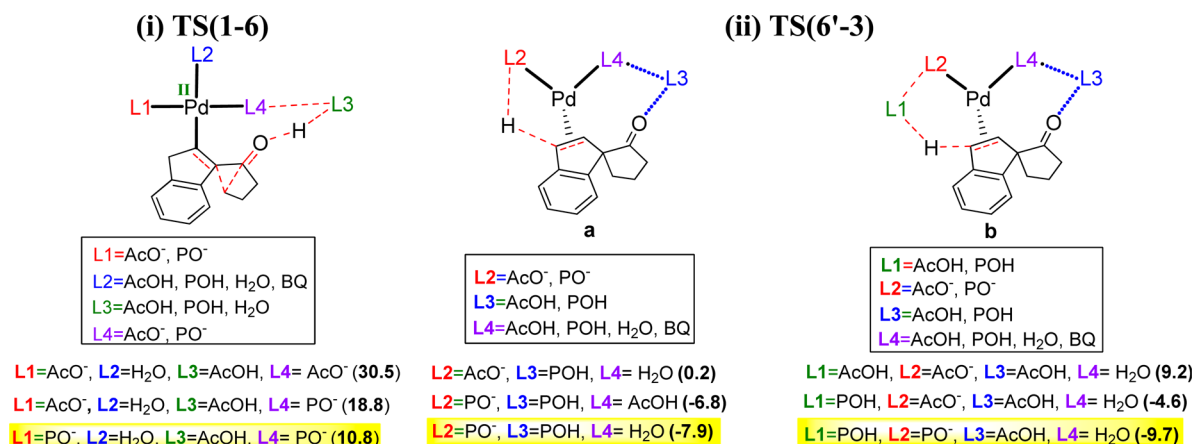


Figure 5. Different possibilities for (i) the ring expansion TS(1-6) and (ii) TS(6'-3) (reductive elimination) in the Wacker type pathway. All ligand combinations considered are provided in the inset while the relative Gibbs free energies (kcal/mol) of the most important TSs are given in parentheses. The reaction coordinate and H-bonding are shown respectively in red and blue colors.

the computed Gibbs free energies of various TSs as given in Figure 4(i) that the most preferred ligands on Pd are BQ and PO⁻ when a second molecule of phosphoric acid (L3) facilitates a relay proton transfer.⁴⁰ BQ is proposed to act as a ligand in allylic C-H activation reaction in some earlier reports.¹⁵ Interestingly, the most favorable ligand combination on palladium (POH and PO⁻) as noticed in the previous C-H bond activation step is found to result in a higher energy TS (11.9 kcal/mol). The geometrical features of TS(2'-3)_{BQ} indicate that the C1-C5 bond formation is accompanied by a concomitant proton transfer from the hydroxyl group to the phosphate oxygen. The conversion of the palladium-bound phosphate to phosphoric acid thus results in the reduction of Pd(II) to Pd(0) in this step.

On the basis of the above descriptions, it is evident that in the allylic pathway, two phosphate ligands are directly involved in the TSs for the C-H activation in the form of a Pd-bound inner-sphere ligand and as an outer-sphere ligand in the subsequent C-C bond formation. More interestingly, the preferred ligands on Pd are found to be water and phosphate in the C-H activation step whereas it is BQ and phosphate in the C-C bond formation. This is an encouraging evidence in line with the concept of "serial ligand catalysis".⁷ If potential ligand exchanges were not invoked, one would have assumed the same type of ligands on palladium throughout the catalytic cycle, leading only to the higher energy mechanistic alternatives. These insights are likely to be helpful in several other transition metal catalyzed reactions, in the presence of various additives and other seemingly innocuous spectator ligands.

Wacker Type Pathway. (i). *Ring Expansion.* An alternative Wacker-type mechanism is examined next, taking into account the key ligand exchanges on Pd, similar to that in the allylic pathway hitherto presented (Figure 5(i)). In the first step of the Wacker pathway, the ring expansion of the cyclobutanol occurs via TS(1-6). The transition state geometry indicates that the C-C bond formation is accompanied by a simultaneous proton transfer from the hydroxyl group to the phosphate oxygen (Figure 6).⁴¹ This proton transfer can either be assisted by an outer-sphere ligand L3, or involve a direct transfer. Akin to the allylic C-H activation TSs described earlier, the most preferred ligand combination turns out to be the one with two phosphate ligands on palladium.⁴² The Gibbs free energy of TS(1-6)_c with a *bis*-phosphate ligand arrange-

ment is 20.3 kcal/mol lower than the conventional *bis*-acetate combination TS(1-6)_a. In the lowest energy TS(1-6)_c, a square planar Pd with two phosphates, a water, and the substrate in an η^1 coordination are found to be the preferred ligands.

(ii). *Reductive Elimination.* In the next step, reductive elimination takes place via TS(6'-3), wherein the C7-H10 is abstracted by either a ligand bound to Pd (mode a) or by an external outer-sphere ligand (mode b) as shown in Figure 5(ii). One of the preferred arrangements for the reductive elimination is found to be when a phosphoric acid ligand moves to an outersphere position to give another intermediate 6'. It can be gleaned from the optimized geometries provided in Figure 6 that the proximity of C7-H10 bond with palladium in 6' induces an agostic interaction (H10-Pd8 distance is 1.82 Å) leading to an elongated C7-H10 (1.20 Å). Upon considering various possible ligand exchanges on Pd for the reductive elimination step, TS(6'-3) is identified as the most preferred mode.⁴³ In this TS, H₂O and PO⁻ act as the bound ligands, while the POH is an external ligand linked through hydrogen bonding, as shown in Figure 6. As a result of C7-H10 deprotonation, C7-C6 bond gains a partial double bond character, which in turn, interacts with palladium. This type of reductive elimination can equally be regarded as a proton coupled electron transfer (PCET) wherein the Pd acts as the electron sink and the proton is abstracted by the phosphate ligand.⁴⁴ In another example, this type of C-H cleavage is described as reductive β -hydride elimination.⁴⁵ It should be noted that a proton, instead of a hydride, is transferred to the phosphate ligand. We have also considered the traditional two-step pathway via TS(6-7) and TS(7-3) involving the formation of a Pd-hydride complex. However, it is found to be of 2.5 kcal/mol higher in energy as compared to the one step reductive elimination process.⁴⁶

Comparison of Allylic C-H Activation and Wacker Type Pathways. A few important insights emerged through the analysis of the most preferred pathways in the allylic and the Wacker-type mechanisms can be noted by examining the comparative energy profiles as given in Figure 7. The free energy profiles clearly indicate that the Wacker-type process is energetically more preferred over the allylic C-H activation pathway. First, the vital transition states in the Wacker pathways are, in general, of lower energy than that in the

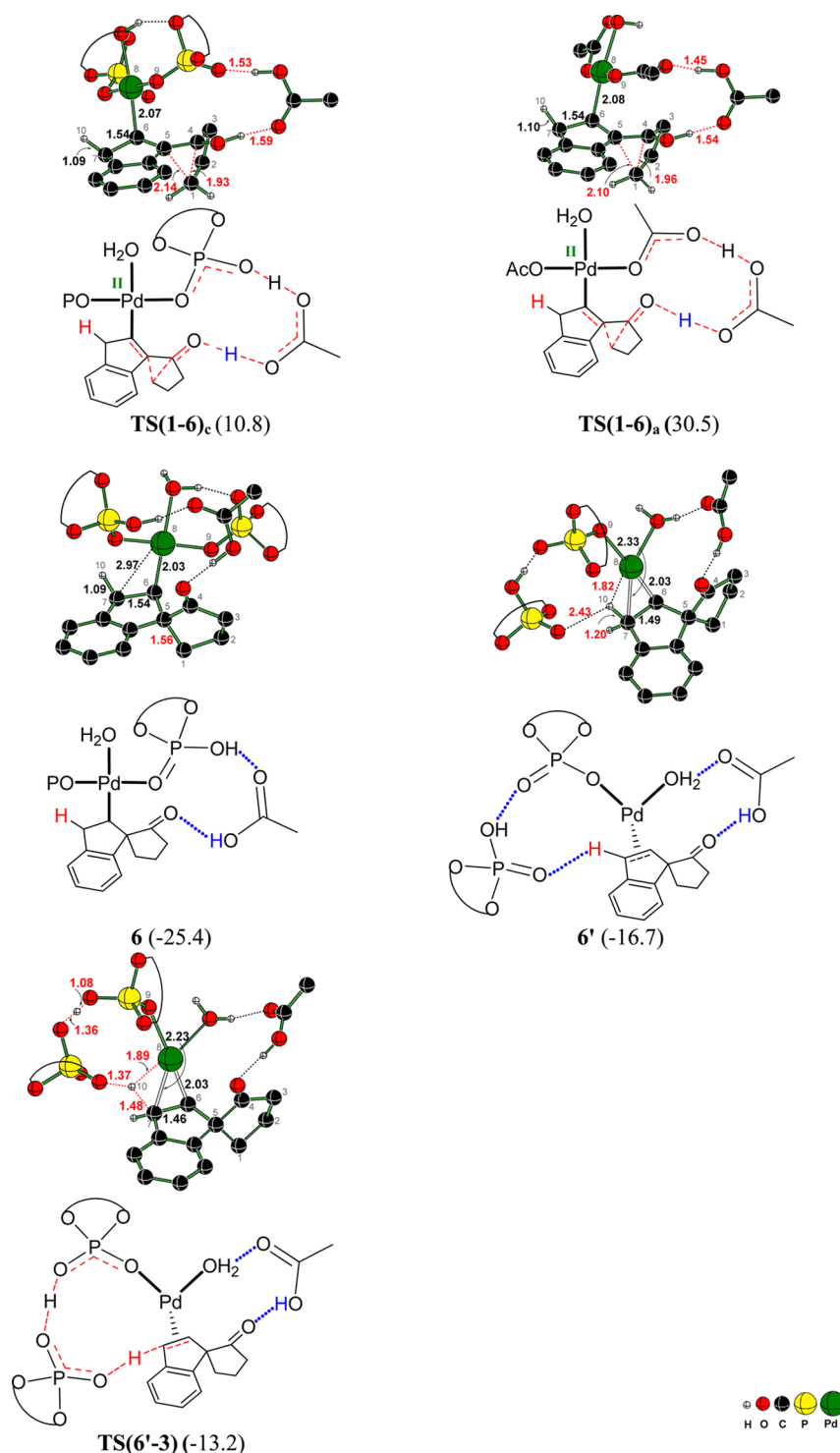


Figure 6. Optimized geometries of important stationary points in the Wacker type process. The relative energies (kcal/mol) are provided in parentheses. All distances are in Å. The reaction coordinate and H-bonding are shown respectively in red and blue colors.

allylic pathway. The very first ring expansion step in the Wacker type pathway (**TS(1-6)_c**) is kinetically more preferred by 7.8 kcal/mol as compared to the first C–H activation step in the allylic pathway (**TS(1-2)_c**). The activation barrier for the second step (**TS(6'-3)**) in the Wacker type pathway is less important in determining the favorability due to the higher stability of intermediate **6**, which makes this process irreversible. On the basis of this analysis, it is evident that the spirocyclic indene formation occurs through a Wacker-type

mechanism with a direct and cooperative participation of phosphoric acid.

In addition, we have compared the efficiency of these two catalytic cycles using the *energetic span* model.⁴⁷ The energetic span, i.e., δE , for the allylic C–H activation pathway is 21.7 kcal/mol and for the Wacker type process is 13.9 kcal/mol. Thus, it is quite evident that the Wacker type pathway will have a higher turnover frequency and is thus expected to be more efficient.⁴⁸

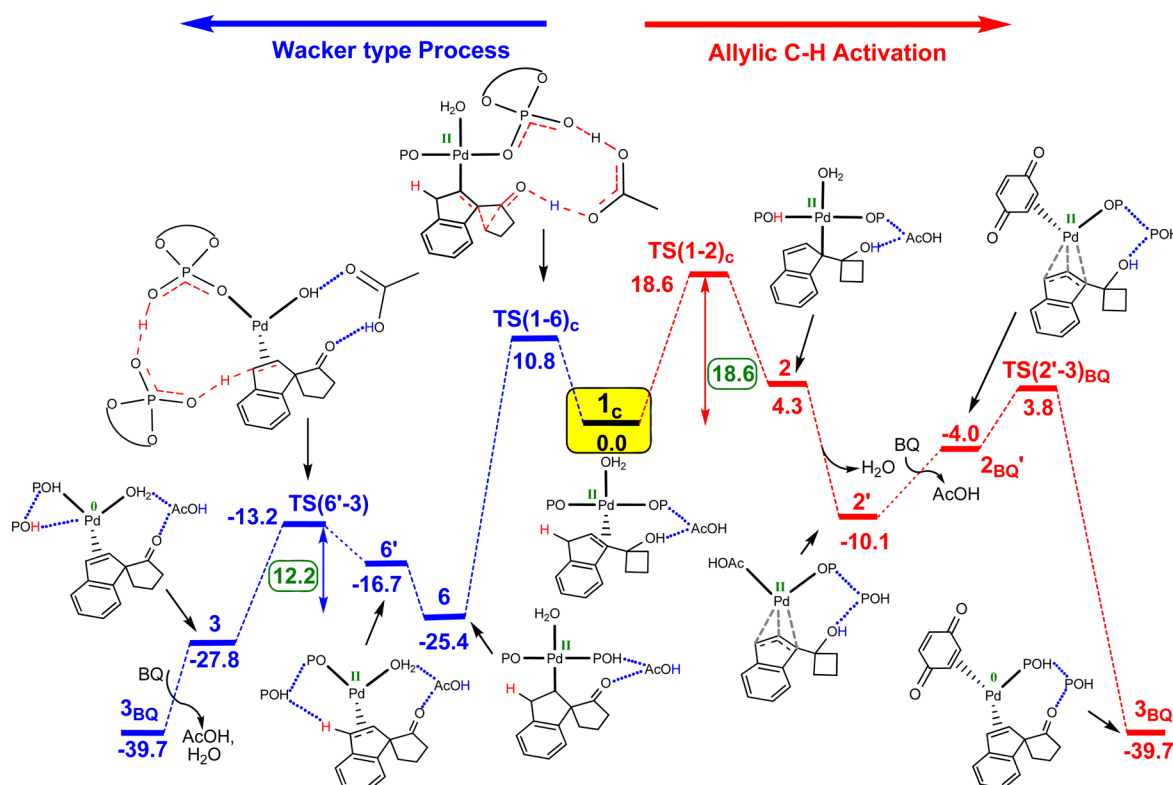


Figure 7. Comparative Gibbs free energy profiles (kcal/mol) for the most preferred pathways in the allylic C–H activation (red) and Wacker type processes (blue).

At this juncture we wish to emphasize the importance of dynamic ligand exchanges in both the mechanistic pathways examined in this study. It can be noticed from the Gibbs free energies of various transition states, as summarized in Table 1,

Table 1. Relative Free Energies (kcal/mol) of the Transition States Involved in the Important Elementary Steps for the Allylic C–H Activation and Wacker Type Pathways with Different Number of Phosphate Ligands on Palladium^a

number of phosphate (PO ⁻) ligands on Pd	allylic C–H activation		Wacker pathway	
	C–H activation	ring expansion	ring expansion	reductive elimination
zero (native)	36.0	20.3	30.5	9.2
one	26.7	10.3	21.5	-4.6
two	18.7	3.8	10.8	-13.2

^aThe activation barriers also follow a similar trend (see Tables S13–S14 in the Supporting Information for more details).

that for all the vital steps of the reaction, replacement of acetate by phosphate offers profound stabilization to the transition states. The *bis*-phosphate ligands on palladium is consistently better for both allylic and Wacker pathways. The higher acidity of phosphoric acid as compared to acetic acid can be regarded as one of the reasons for this observation. The pK_a of the Brønsted acid catalyst (**I**) employed is 3.58, whereas that of acetic acid is 12.6 (both in DMSO). Thus, phosphoric acid can protonate the palladium-bound acetate. The transition state for this process is found to have an activation barrier of only 4 kcal/mol, suggesting that this process is indeed a facile one.^{33g} It is interesting to note that in the allylic C–H activation pathway, BQ acts as a more preferred ligand in the transition state for the C–C bond formation leading to the ring

expansion. However, in the lower energy Wacker-type process, BQ is not a preferred ligand in both the C–C bond formation and the reductive elimination. It is therefore evident that BQ plays the role of an oxidant in the regeneration of the catalyst rather than participating in ligand exchanges in the preceding steps of the title reaction.³⁰

Potential Involvement of Palladium Phosphate as an Active Catalyst for Other C–H Activation Reactions. On the basis of the discussions presented in the previous sections, it is quite evident that the palladium phosphate (Pd(OP)₂) generated *in situ* by the action of phosphoric acid on the native palladium acetate (Pd(OAc)₂) can act as a better active catalyst. We became curious to examine whether an extension of this concept to other Pd(OAc)₂ catalyzed reactions may well become valid. In this regard, we have investigated the potential role of (Pd(PMe₃)Ph(OP)) in the C–H activation of a series of arenes that were earlier reported with Pd(PMe₃)Ph(OAc).⁴⁹ The palladium-bound acetate in the C–H activation TSs was replaced with a phosphate and geometries were reoptimized. The relative free energies as summarized in Table 2 reveals that for all the four substrates, the transition states with phosphate are lower as compared to the corresponding acetates. Thus, the prediction that a phosphate assisted C–H activation is energetically more preferred over the acetate assisted C–H activation, appears to hold good across different types of reactions as well.

CONCLUSIONS

The mechanism of formation of spirocyclic indenes using a cooperative multicatalytic protocol involving palladium acetate and phosphoric acid is established using density functional theory computational methods. Of the two important

Table 2. Comparison of the Relative Free Energies (kcal/mol) for Ligand Assisted Arene C–H Activation using Palladium acetate and Palladium phosphate

Ar				
	0.0	0.0	0.0	0.0
	-4.9	-5.4	-3.4	-4.2

mechanistic alternatives examined, a Wacker-type pathway consisting of a semipinacol ring expansion of the indenyl cyclobutanol followed by a reductive elimination (proton coupled electron transfer) leading to a spirocyclic indene, is found to be more preferred over an alternative route via an allylic C–H activation pathway. Ligand exchange has been identified as vital toward identifying the lower energy mechanistic pathways, wherein the replacement of the native acetate ligands on palladium by phosphate as well as water resulted in additional stabilization of the crucial transition states. These transition states are profoundly lower in energies in both the allylic C–H activation pathway and in the Wacker type process. As a consequence, an interesting phosphate assisted C–H activation has been identified as more preferred over the commonly invoked acetate assisted route. Further, in the ring expansion transition state in the allylic pathway, a molecule of benzoquinone and a phosphate are found to be the most favored ligands on palladium. In the energetically favored Wacker type pathway, the most preferred arrangement for the ring expansion step has been identified as the one wherein phosphates are bound to palladium as a ligand. In this process, the cyclobutanol proton is abstracted first by an outer-sphere acetate before it is relayed to the phosphate ligand. In the next step, the phosphoric acid remains in the outer-sphere and relays the indenyl β -proton to the palladium-bound phosphate. Thus, Brønsted acid has been identified as playing a dual role in the overall Wacker type mechanism. Further studies aimed at establishing the origin of enantioselectivity in the formation of the spirocyclic indenenes are currently underway.

■ ASSOCIATED CONTENT

Supporting Information

Optimized geometries, additional schemes, figures, and tables are provided. This material is available free of charge via the Internet at <http://pubs.acs.org>.

■ AUTHOR INFORMATION

Corresponding Author

sunoj@chem.iitb.ac.in

Notes

The authors declare no competing financial interest.

■ ACKNOWLEDGMENTS

Generous computing time from IIT Bombay supercomputing facility and National Nanotechnology Infrastructure Network (NNIN) at Michigan are acknowledged. We acknowledge Prof. Trevor J. Rainey (Montana State University, Bozeman) for some valuable discussions during the late stages of our mechanistic study. Research funding from BRNS (Mumbai) under the basic sciences scheme is acknowledged. G.J. is grateful to CSIR-New Delhi for a Senior Research Fellowship.

■ REFERENCES

- (1) (a) Hartwig, J. F. *Nature* **2008**, *455*, 314. (b) Ritleng, V.; Sirlin, C.; Pfeffer, M. *Chem. Rev.* **2002**, *102*, 1731. (c) Bergman, R. G. *Nature* **2007**, *446*, 391. (d) Godula, K.; Sames, D. *Science* **2006**, *312*, 67. (e) Chen, M. S.; White, M. C. *Science* **2007**, *318*, 783. (f) Chen, K.; Baran, P. S. *Nature* **2009**, *459*, 824. (g) Balcells, D.; Clot, E.; Eisenstein, O. *Chem. Rev.* **2010**, *110*, 749.
- (2) Park, Y. J.; Park, J.-W.; Jun, C.-H. *Acc. Chem. Res.* **2008**, *41*, 222.
- (3) (a) Xu, H.; Zeund, S. J.; Woll, M. G.; Tao, Y.; Jacobsen, E. N. *Science* **2010**, *327*, 986. (b) Rueping, M.; Koenigs, R. M.; Atodiresci, I. *Chem.—Eur. J.* **2010**, *16*, 9350. (c) Paull, D. H.; Abraham, C. J.; Scerba, M. T.; Alden-Danforth, E.; Lectka, T. *Acc. Chem. Res.* **2008**, *41*, 655. (d) Raup, D. E. A.; Cardinal-David, B.; Holte, D.; Scheidt, K. A. *Nat. Chem.* **2010**, *2*, 766. (e) Park, J.; Hong, S. *Chem. Soc. Rev.* **2012**, *41*, 6931. (f) Du, Z.; Shao, Z. *Chem. Soc. Rev.* **2013**, *42*, 1337. (g) Zhong, C.; Shi, X. *Eur. J. Org. Chem.* **2010**, 2999. (h) Shao, Z.; Zhang, H. *Chem. Soc. Rev.* **2009**, *38*, 2745. (i) Chen, D.-F.; Han, Z.-Y.; Zhou, X.-L.; Gong, L.-Z. *Acc. Chem. Res.* **2014**, *47*, 2365.
- (4) (a) Fors, B. P.; Buchwald, S. L. *J. Am. Chem. Soc.* **2010**, *132*, 15914. (b) Stmabuli, J. P.; Incarvito, C. D.; Bühl, M.; Hartwig, J. F. *J. Am. Chem. Soc.* **2004**, *126*, 1184. (c) Cheng, G.-J.; Yang, Y.-F.; Liu, P.; Chen, P.; Sun, T.-Y.; Li, G.; Zhang, X.; Houk, K. N.; Yu, J.-Q.; Wu, Y.-D. *J. Am. Chem. Soc.* **2014**, *136*, 894. (d) Maleckis, A.; Kampf, J. W.; Sanford, M. S. *J. Am. Chem. Soc.* **2013**, *135*, 6618. (e) Richens, D. T. *Chem. Rev.* **2005**, *105*, 1961. (f) Shekhar, S.; Ryberg, P.; Hartwig, J. F.; Mathew, J. S.; Blackmond, D. G.; Strieter, E. R.; Buchwald, L. S. *J. Am. Chem. Soc.* **2006**, *128*, 3584. (g) Kalek, M.; Stawinski, J. *Organometallics* **2008**, *27*, 5876. (h) Chen, T.; Guo, C.; Goto, M.; Han, L.-B. *Chem. Commun.* **2013**, *49*, 7498. (i) Cong, X.; Tang, H.; Wu, C.; Zeng, X. *Organometallics* **2013**, *32*, 6565.
- (5) Engle, K. M.; Yu, J.-Q. *J. Org. Chem.* **2013**, *78*, 8927.
- (6) Chai, Z.; Rainey, T. J. *J. Am. Chem. Soc.* **2012**, *134*, 3615.
- (7) (a) Reed, S. A.; White, M. C. *J. Am. Chem. Soc.* **2008**, *130*, 3316. (b) Fraunhoffer, K. J.; White, M. C. *J. Am. Chem. Soc.* **2007**, *129*, 7274. (c) Chen, M. S.; Prabakaran, N.; Labenz, N. A.; White, M. C. *J. Am. Chem. Soc.* **2005**, *127*, 6970. (d) Liu, G.; Yin, G.; Wu, L. *Angew. Chem., Int. Ed.* **2008**, *47*, 4733. (e) Lin, S.; Song, C.-X.; Cai, G.-X.; Wang, W.-H.; Shi, Z.-J. *J. Am. Chem. Soc.* **2008**, *130*, 12901. (f) Campbell, A. N.; White, P. B.; Guzei, I. A.; Stahl, S. S. *J. Am. Chem. Soc.* **2010**, *132*, 15116.
- (8) (a) This is in contrast to the allylic alkylation with prefunctionalized substrates. (b) The *ees* obtained in the acetoxylation (C–O bond formation) reaction using a chiral Lewis acid were only modest (~60%). See: Covell, D. J.; White, C. *Angew. Chem., Int. Ed.* **2008**, *47*, 6448.
- (9) (a) Wang, B.; Tu, Y. Q. *Acc. Chem. Res.* **2011**, *44*, 1207. (b) Franz, A. K.; Hanhan, N. V.; Ball-Jones, N. *ACS Catal.* **2013**, *3*, 540. (c) Zhang, Q.-W.; Fan, C.-A.; Zhang, H.-J.; Tu, Y.-Q.; Zhao, Y.-M.; Gu, P.; Chen, Z.-M. *Angew. Chem., Int. Ed.* **2009**, *48*, 8572. (d) D'yakov, V. A.; Trapeznikova, O. A.; de Meijere, A.; Dzhemilev, U. M. *Chem. Rev.* **2014**, *114*, 5775.
- (10) (a) Abel, U.; Simon, W.; Eckard, P.; Hansske, F. G. *Bioorg. Med. Chem. Lett.* **2006**, *16*, 3292. (b) Kita, Y.; Higuchi, K.; Yoshida, Y.; Iio, K.; Kitagaki, S.; Akai, S.; Fujioka, H. *Angew. Chem., Int. Ed.* **1999**, *38*, 683. (c) Kita, Y.; Higuchi, K.; Yoshida, Y.; Iio, K.; Kitagaki, S.; Ueda, K.; Akai, S.; Fujioka, H. *J. Am. Chem. Soc.* **2001**, *123*, 3214. (d) Li, F.; Tartakoff, S. S.; Castle, S. L. *J. Am. Chem. Soc.* **2009**, *130*, 6674.

- (11) (a) Yip, K.-T.; Nimje, R. Y.; Leskinen, M. V.; Pihko, P. M. *Chem.—Eur. J.* **2012**, *18*, 12590. (b) Nahra, F.; Liron, F.; Prestat, G.; Mealli, C.; Messaoudi, A.; Poli, G. *Chem.—Eur. J.* **2009**, *15*, 11078. (c) Zhang, S.-Y.; He, G.; Nack, W. A.; Zhao, Y.; Li, Q.; Chen, G. *J. Am. Chem. Soc.* **2013**, *135*, 2124.
- (12) Yu, S.-Y.; Zhang, H.; Gao, Y.; Mo, L.; Wang, S.; Yao, Z.-J. *J. Am. Chem. Soc.* **2013**, *135*, 11402.
- (13) Osberger, T. J.; White, M. C. *J. Am. Chem. Soc.* **2014**, *136*, 11176.
- (14) Xiong, T.; Li, Y.; Mao, L.; Zhang, Q.; Zhang, Q. *Chem. Commun.* **2012**, *48*, 2246.
- (15) (a) Lyons, T. W.; Hull, K. L.; Sanford, M. S. *J. Am. Chem. Soc.* **2011**, *133*, 4455. (b) Sköld, C.; Kleimark, J.; Trejos, A.; Odell, L. R.; Nilsson Lill, S. O.; Norrby, P.-O.; Larhed, M. *Chem.—Eur. J.* **2012**, *18*, 4714.
- (16) Liron, F.; Oble, J.; Lorion, M. M.; Poli, G. *Eur. J. Org. Chem.* **2014**, 5863.
- (17) (a) Anand, M.; Sunoj, R. B. *Org. Lett.* **2011**, *13*, 4802. (b) Jindal, G.; Sunoj, R. B. *Chem.—Eur. J.* **2012**, *18*, 7045. (c) Anand, M.; Sunoj, R. B. *Organometallics* **2012**, *31*, 6466. (d) Anand, M.; Sunoj, R. B. *Org. Lett.* **2012**, *14*, 4584. (e) Parija, A.; Sunoj, R. B. *Org. Lett.* **2012**, *15*, 4066. (f) Jindal, G.; Sunoj, R. B. *Angew. Chem., Int. Ed.* **2014**, *53*, 4432. (g) Jindal, G.; Sunoj, R. B. *Org. Biomol. Chem.* **2014**, *12*, 2745. (h) Anand, M.; Sunoj, R. B.; Schaefer, H. F. *J. Am. Chem. Soc.* **2014**, *136*, 5535. (i) Jindal, G.; Sunoj, R. B. *J. Org. Chem.* **2014**, *79*, 7600.
- (18) Frisch, M. J.; Trucks, G. W.; Schlegel, H. B.; Scuseria, G. E.; Robb, M. A.; Cheeseman, J. R.; Scalmani, G.; Barone, V.; Mennucci, B.; Petersson, G. A.; Nakatsuji, H.; Caricato, M.; Li, X.; Hratchian, H. P.; Izmaylov, A. F.; Bloino, J.; Zheng, G.; Sonnenberg, J. L.; Hada, M.; Ehara, M.; Toyota, K.; Fukuda, R.; Hasegawa, J.; Ishida, M.; Nakajima, T.; Honda, Y.; Kitao, O.; Nakai, H.; Vreven, T.; Montgomery, J. A., Jr.; Peralta, J. E.; Ogliaro, F.; Bearpark, M.; Heyd, J. J.; Brothers, E.; Kudin, K. N.; Staroverov, V. N.; Kobayashi, R.; Normand, J.; Raghavachari, K.; Rendell, A.; Burant, J. C.; Iyengar, S. S.; Tomasi, J.; Cossi, M.; Rega, N.; Millam, N. J.; Klene, M.; Knox, J. E.; Cross, J. B.; Bakken, V.; Adamo, C.; Jaramillo, J.; Gomperts, R.; Stratmann, R. E.; Yazyev, O.; Austin, A. J.; Cammi, R.; Pomelli, C.; Ochterski, J. W.; Martin, R. L.; Morokuma, K.; Zakrzewski, V. G.; Voth, G. A.; Salvador, P.; Dannenberg, J. J.; Dapprich, S.; Daniels, A. D.; Farkas, Ö.; Foresman, J. B.; Ortiz, J. V.; Cioslowski, J.; Fox, D. J. *Gaussian 09*, Revision A.02; Gaussian, Inc.: Wallingford, CT, 2009.
- (19) (a) Hehre, W. J.; Ditchfield, R.; Pople, J. A. *J. Chem. Phys.* **1972**, *56*, 2257. (b) Hariharan, P. C.; Pople, J. A. *Theor. Chim. Acta* **1973**, *28*, 213. (c) Lee, C.; Yang, W.; Parr, R. G. *Phys. Rev. B: Condens. Matter Mater. Phys.* **1988**, *37*, 785. (d) Becke, A. D. *J. Chem. Phys.* **1993**, *98*, 5648.
- (20) Hay, P. J.; Wadt, W. R. *J. Chem. Phys.* **1985**, *82*, 299.
- (21) (a) Gonzalez, C.; Schlegel, H. B. *J. Chem. Phys.* **1989**, *90*, 2154. (b) Gonzalez, C.; Schlegel, H. B. *J. Phys. Chem.* **1990**, *94*, 5523.
- (22) (a) Zhao, Y.; Truhlar, D. G. *Theor. Chem. Acc.* **2008**, *120*, 215. (b) Zhao, Y.; Truhlar, D. G. *Acc. Chem. Res.* **2008**, *41*, 157. (c) Zhao, Y.; Truhlar, D. G. *Org. Lett.* **2007**, *9*, 1967.
- (23) (a) Liu, P.; Xu, X.; Dong, X.; Keitz, B. K.; Herbert, M. B.; Grubbs, R. H.; Houk, K. N. *J. Am. Chem. Soc.* **2012**, *134*, 1464. (b) Komagawa, S.; Wang, C.; Morokuma, K.; Saito, S.; Uchiyama, M. *J. Am. Chem. Soc.* **2013**, *135*, 14508. (c) Wang, Z. J.; Benitez, D.; Tkatchouk, E.; Goddard, W. A., III; Toste, F. D. *J. Am. Chem. Soc.* **2010**, *132*, 13064. (d) Biswas, S.; Huang, Z.; Choliy, Y.; Wang, D. Y.; Brookhart, M.; Krogh-Jespersen, K.; Goldman, A. S. *J. Am. Chem. Soc.* **2012**, *134*, 13276.
- (24) Marenich, A. V.; Cramer, C. J.; Truhlar, D. G. *J. Phys. Chem. B* **2009**, *113*, 6378.
- (25) (a) Tamura, H.; Yamasaki, H.; Sato, H.; Sakaki, S. *J. Am. Chem. Soc.* **2003**, *125*, 16114. (b) Sakaki, S.; Takayama, T.; Sumimoto, M.; Sugimoto, M. *J. Am. Chem. Soc.* **2004**, *126*, 3332. (c) Braga, A. A. C.; Ujaque, G.; Maseras, F. *J. Am. Chem. Soc.* **2006**, *25*, 3647. (d) Tanaka, R.; Yamashita, M.; Chung, L. W.; Morokuma, K.; Nozaki, K. *Organometallics* **2011**, *30*, 6742.
- (26) (a) Benson, S. W. *The Foundations of Chemical Kinetics*; R. E. Krieger: Malabar, FL, 1982. (b) Okuno, Y. *Chem.—Eur. J.* **1997**, *3*, 210. (c) Ardura, D.; López, R.; Sordo, T. L. *J. Phys. Chem. B* **2005**, *109*, 23618. (d) Liu, Q.; Lan, Y.; Liu, J.; Li, G.; Wu, Y.-D.; Lei, A. *J. Am. Chem. Soc.* **2009**, *131*, 10201. (e) Ariafard, A.; Brookes, N. J.; Stranger, R.; Yates, B. F. *Organometallics* **2011**, *30*, 1340.
- (27) (a) Mammen, M.; Shakhnovich, E. I.; Deutch, J. M.; Whitesides, G. M. *J. Org. Chem.* **1998**, *63*, 3821. (b) Ishikawa, A.; Nakao, Y.; Sato, H.; Sakaki, S. *Inorg. Chem.* **2009**, *48*, 8154. (c) Sakata, K.; Fujimoto, H. *J. Org. Chem.* **2013**, *78*, 12505. (d) Zeng, G.; Li, S. *Inorg. Chem.* **2011**, *50*, 10572. (e) Zhang, W.; Moore, J. S. *J. Am. Chem. Soc.* **2005**, *127*, 11863.
- (28) The corrected free energies using the Whitesides method are given in Tables S1–S13 as ΔG_{corr} .
- (29) The energetic details are provided in Table S11 in the Supporting Information.
- (30) Engelin, C. J.; Jensen, T.; Rodríguez-Rodríguez, S.; Fristrup, P. *ACS Catal.* **2013**, *3*, 294.
- (31) (a) Liu, L.; Yuan, T.; Wang, T.; Gao, X.; Zeng, Z.; Zhu, J.; Zhao, Y. *J. Org. Chem.* **2014**, *79*, 80. (b) Liu, L.; Wu, Y.; Wang, T.; Gao, X.; Zhu, J.; Zhao, S. *J. Org. Chem.* **2014**, *79*, S074.
- (32) It should be noted that the position of the ligands and the conformation could vary. Higher energy conformers are provided in Table S1 in the Supporting Information.
- (33) The trimeric Pd₃(OAc)₆ is chosen as the reference point because palladium(II) acetate is known to exist as a trimer in benzene and CH₂Cl₂. See (a) Stephens, T. A.; Morehous, S. M.; Powell, A. R.; Heffer, J. P.; Wilkinson, G. *J. Chem. Soc.* **1965**, 3632. (b) Bakhtmutov, V. I.; Berry, J. F.; Cotton, F. A.; Ibragimov, S.; Murillo, C. A. *Dalton Trans.* **2005**, 1989. (c) Giri, R.; Lan, Y.; Liu, P.; Houk, K. N.; Yu, J.-Q. *J. Am. Chem. Soc.* **2012**, *134*, 14118. (d) Nosova, V. M.; Ustynyuk, Y. U.; Bruk, L. G.; Temkin, O. N.; Kisin, A. V.; Storozhenko, P. A. *Inorg. Chem.* **2011**, *50*, 9300. (e) Skapskia, A. C.; Smart, M. L. *Chem. Commun.* **1970**, 658. (f) Adrio, L. A.; Nguyen, B. N.; Guilera, G.; Livingston, A. G.; Hii, K. K. *Catal. Sci. Technol.* **2012**, *2*, 316. (g) See Scheme S1 in the Supporting Information for more details.
- (34) Additional details pertaining to the inclusion of two explicit AcOH molecules in the transition states are given in Table S15 in the Supporting Information.
- (35) The details of other higher energy TSs with varying ligand combinations are provided in Tables S4, S5 in the Supporting Information.
- (36) See Tables S2, S3 in the Supporting Information for full details.
- (37) Interesting reports on ligand assisted C–H activations, See (a) Engle, K. M.; Wang, D.-H.; Yu, J.-Q. *J. Am. Chem. Soc.* **2010**, *132*, 14137. (b) Ackermann, L. *Chem. Rev.* **2011**, *111*, 1315. (c) Lafrance, M.; Rowley, C. N.; Woo, T. K.; Fagnou, K. *J. Am. Chem. Soc.* **2006**, *128*, 8754. (d) Davies, S. S.; Donald, D. L.; A, S. M.; Macgregor, S. A. *J. Am. Chem. Soc.* **2005**, *127*, 13754.
- (38) (a) Jiang, G.; Halder, R.; Fang, Y.; List, B. *Angew. Chem., Int. Ed.* **2011**, *50*, 9752. (b) Tao, Z.-L.; Zhang, W.-Q.; Chen, D.-F.; Adele, A.; Gong, L.-Z. *J. Am. Chem. Soc.* **2013**, *135*, 9255. (c) In a very recent example, a Pd- π -allyl-phosphate was detected using HRMS and even employed as a catalyst. See: Zhang, D.; Qiu, H.; Jiang, L.; Lv, F.; Ma, C.; Hu, W. *Angew. Chem., Int. Ed.* **2013**, *52*, 13356.
- (39) See Table S10 in the Supporting Information for other higher energy intermediates.
- (40) (a) Details of TSs involving other ligand combinations and direct proton transfer are given in Table S6 in the Supporting Information. (b) NBO analysis is done to ascertain the nature of bonding between BQ and Pd and its favorable role as a ligand. See Table S12 in the Supporting Information.
- (41) The IRC calculations followed by geometry optimization of the end point using “opt=calcfc” led to intermediate 6.
- (42) For other ligand combinations of higher energy see Table S7 in the Supporting Information. An additional TS involving a proton relay via two explicit AcOH molecules is located and is found to be of 2.8 kcal/mol higher in energy than TS(1–6).

(43) For other ligand combinations of higher energy see Tables S8, S9 in the Supporting Information.

(44) For studies that describe the C–H cleavage as PCET, see:
(a) Leskinen, M. V.; Madarász, A.; Yip, K.-T.; Vuorinen, A.; Pápai, I.; Neuvonen, A. J.; Pihko, P. M. *J. Am. Chem. Soc.* **2014**, *136*, 6453.

(b) Seu, C. S.; Appel, A. M.; Doud, M. D.; DuBois, D. L.; Kubiak, C. P. *Energy Environ. Sci.* **2012**, *5*, 6480.

(45) Nielsen, R. J.; Goddard, W. A., III *J. Am. Chem. Soc.* **2006**, *128*, 9651.

(46) See Scheme S4 and Figure S2 in the Supporting Information for more details.

(47) Kozuch, S.; Shaik, S. *Acc. Chem. Res.* **2011**, *44*, 101. For more details see Figure S3 in Supporting Information.

(48) It should be noted that within the Wacker type process it is difficult to identify the rate determining state due to the close values of δE . For the ring expansion δE is 13.9 kcal/mol, whereas for the reductive elimination it is 12.8 kcal/mol.

(49) We thank an anonymous referee for prompting us to examine some of the related arene C–H activation reactions. Petit, A.; Flygare, J.; Miller, A. T.; Winkel, G.; Ess, D. H. *Org. Lett.* **2012**, *14*, 3680.